Poiseuille flow in a nanochannel – use of different thermostats

A. Ghosh[1], R. Paredes[2], S. Luding[1]

[1)] Nanostructured Materials, DelftChemTech. Julianalaan 136, 2628 BL Delft, Netherlands
[2)] Centro de Física, Inst. Venez. de Invest. Científicas, Apdo. 21827, Caracas 1020 A Venezuela

ABSTRACT

Poiseuille flow of a liquid in a nano-channel is simulated by molecular dynamics by embedding the fluid particles in a uniform force field. The channel is periodic in y and z directions and along x direction it is bounded by atomic walls. The imposition of the body force generates heat in the system leading to shear heating and a non-uniform temperature rise across the channel. In this nonequilibrium system, one can attempt to control temperature in different ways: velocity rescaling, thermostats or wall-fluid coupling. We evaluate and compare different methods critically by analyzing the fluctuations and time averaged quantities from various simulations. When particles will be inserted into the flow, it is expected that the dynamics will depend on the thermostat chosen. First observations show little influence of the thermostats on single tracer particles – this needs further study.

INTRODUCTION

In many non-equilibrium fluid systems [1], like pressure driven fluid flows [2] or sheared liquid films [3] in nano-geometries [4], flow energy is converted into thermal energy, resulting in a temperature increase. Especially the boundary conditions of such systems are an issue under discussion [3-6], since the walls couple to the environment that is possibly in thermal equilibrium, while the fluid in the channel is not. In these situations, often a constant temperature condition can be desirable, which requires the dissipation of the excess energy. In molecular dynamics simulations several ways of thermostatting a system exist [1-7] – some of these are velocity rescaling, Nose Hoover or Anderson thermostats, and the use of velocity- and/or position-dependent forces.

In this study, we simulate by molecular dynamics a body force driven flow of a model liquid interacting via the well-known [1] 12-6 Lennard Jones potential:

$$V_{LJ} = 4\,\varepsilon\,\left[\,(\sigma/r)^{12} - (\sigma/r)^{6}\,\right],$$

where ε is the interaction strength (energy) and σ is the (typical) diameter of the particles, in a nano-sized slit. The effect of the (artificial) thermostats on the dynamics of the systems is examined and different thermostats are critically evaluated by comparing the fluctuations and the time-averaged quantities – temperature, velocity profiles, and velocity distributions – at different flow rates.

MODEL SYSTEM

In the present simulations, σ, ε and m are the units of length, energy and mass, respectively. Other units can be expressed in terms of these units, e.g., the temperature T=1, corresponds to 119K and time t=1 to 2.14×10^{-12}s. The time-step used for our simulations is dt=0.001. The fluid-fluid, fluid-wall and wall-wall interaction strengths ε and diameters σ are all identically equal to unity $\varepsilon = \sigma = 1.0$.

The density and temperature of the system are $\nu = N\pi\sigma^3/(6V) = 0.8$ and T=1.0, respectively, with N fluid atoms and fluid volume V.

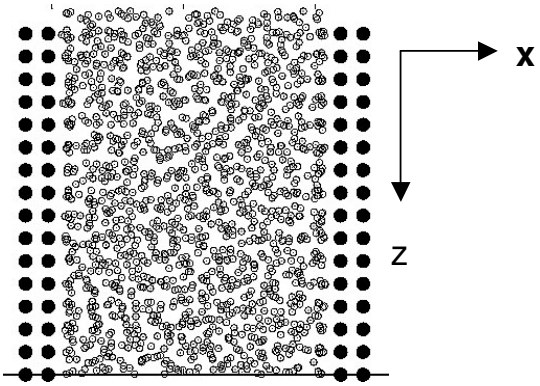

Fig.1: Snapshot in x-z projection. Solid circles represent the wall particles. The distance between the two walls is 11σ. The fluid particles (open circles) are flowing along the downward z-direction.

As sketched in Fig.1, the fluid particles are flowing through a narrow channel, where along y (out-of-plane) and the z directions periodic boundary conditions are applied. In x-direction, the system is bounded by walls, composed of two 001 fcc (square) layers, made of 128 particles each. The channel width, i.e., the separation between the inner walls, is 11.1σ, and the wall-particle distance is 1.71σ. The height and depth of the system are 13.67σ, and the number of fluid particles is N=1536.

Different Thermostats

In the simplest model, the wall atoms are assumed to have infinite mass and therefore remain static at their original positions throughout the simulation. This does not allow for heat exchange or control via the walls. In this case, thermostats that artificially extract heat from the system e.g., velocity rescaling or velocity dependent forces (Nose-Hoover – local as well as global) are used, together with the Velocity Verlet method for integration of the trajectories of the particles.

For *velocity rescaling*, the velocities are first updated from the forces acting on the particles and then rescaled at each time step according to:

$$\phi = (T_{select} / T_{inst})^{1/2}, \qquad (1.1)$$

$$v_i = (1-\phi)v_{icm} + \phi v_i, \qquad (1.2)$$

where T_{select} is the target temperature and T_{inst} the instantaneous (global) temperature of all fluid particles in the system. The temperature is defined here as fluctuation kinetic energy (the mean velocity has to be disregarded) per particle, per degree of freedom:

$$T_{inst} := kT = 2E/3mN = \left[\left\langle v_x^2 \right\rangle + \left\langle v_y^2 \right\rangle + \left\langle v_z^2 \right\rangle\right]/3 \ .$$

For a *Nose Hoover thermostat* [1], the equation of motion of particle *i* is given by:

$$\frac{dp_i}{dt} = m_i b_z + F_{\text{int}} + \xi p_i, \qquad (1.3)$$

with the force on a particle due to pair-interactions, $F_{\text{int}} = F(r) - F(r_c)$, with $F(r) = -\partial V_{\text{LJ}}/\partial r$, and the LJ cut-off radius $r_c = 2.5\sigma$, a body force in z-direction $m_i b_z$, and a time dependent friction coefficient

$$\dot{\xi} = (\sum_i p_i^2 / m_i - L/\beta)/Q \ , \qquad (1.4)$$

where p_i and m_i are the momentum and the mass of the i th particle. Here L=3N and β = 1/T and Q is the thermostat scale factor.

RESULTS

Poiseuille flow is simulated in the system by imposing a constant gravity like force along the z direction on each fluid particle. Since the system is highly dense (0.8) and small in size (~nm) any local fluctuation propagates quickly through the system; so does also the temperature inserted in the areas of high shear rate close to the walls. In the free heating mode, i.e., in absence of any of the thermostats, the heating leads to an increasing temperature and a uniform temperature distribution across the channel, besides fluctuations, as shown in Fig. 2. The inset indicates a slightly super-linear increase of temperature with time while the main figure shows the density and temperature profile at a certain time. The statistics is rather bad since, due to the increasing temperature, one can average only over a very short time-interval.

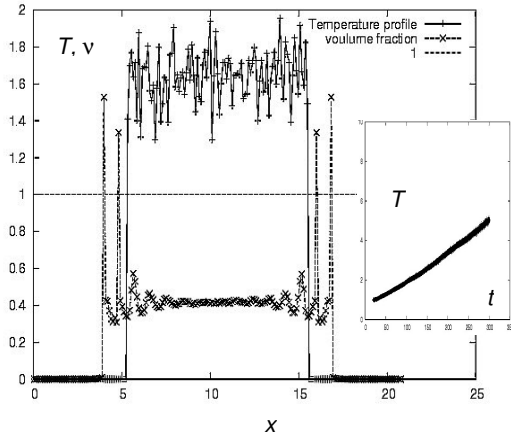

Fig.2: Temperature and density profiles across the channel averaged over 20 files recorded at an interval of 10 iteration steps. The dashed horizontal line shows the initial temperature T=1 of the system. *Inset*: Temperature T as function of time t in absence of any thermostat – with body force bz=0.1

Thus one reason to thermostat a system is to allow for time-averages over many snapshots when the temperature is kept constant. Figs. 3, and 4 show the temperature fluctuations for both Nose-Hoover thermostat and velocity rescaling.

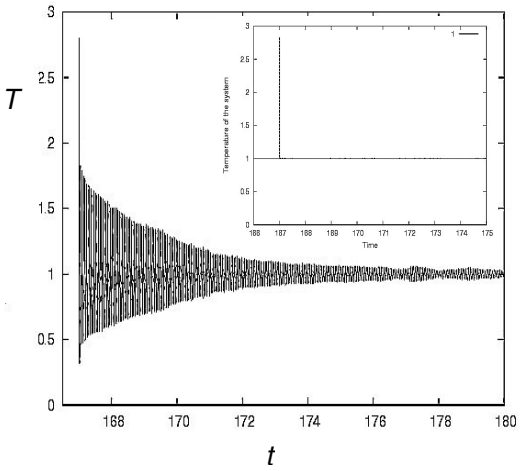

Fig.3 Temperature fluctuations (initial value T=2.8) for the Nose-Hoover thermostat as function of time with Q=1.0. Smaller Q values lead to faster relaxation and vice-versa (data not shown). *Inset*: The same for the velocity rescaling – the adaptation to the desired temperature is immediately taking place after one time-step.

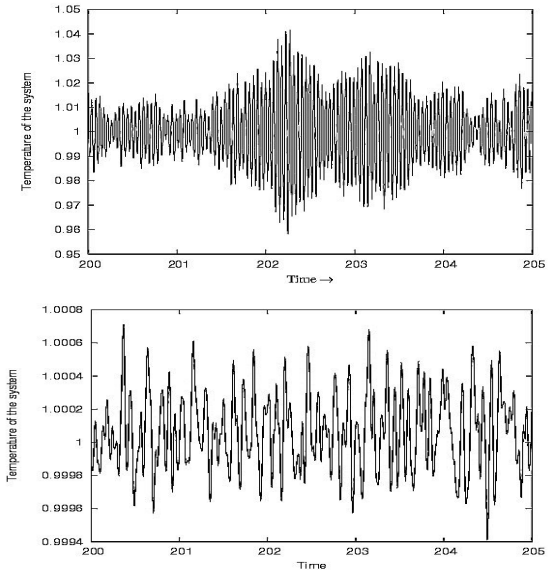

Fig.4: Temperature as function of time. Top and bottom figures correspond to Nose-Hoover and velocity rescaling – some time later than in Fig.3. The data points are taken at the same frequency and over the same time-interval to allow for a comparison. Note that the vertical axis scaling is different.

The variation of temperature with time is shown in Figs.3 and 4 for both thermostatting methods. The initial temperature of the system is 2.8 and with the application of the thermostats it decays down to the target-temperature T=1, see Fig. 3. The Nose-Hoover thermostat takes a finite time of around t=10, whereas velocity rescaling changes the temperature in a single step to a value very close to the target T.

From Fig.4, we learn that velocity rescaling shows more random fluctuations with much smaller amplitude. Nose–Hoover leads to rather periodic oscillations indicating the presence of certain well-defined frequencies. A more detailed Fourier analysis is far from the scope of this paper. Note, however, that the Nose-Hoover thermostat has the advantage that it does not depend on the numerical time-step, whereas for velocity rescaling, a smaller time-step leads to smaller fluctuation amplitudes.

Remarkably, the differences in relaxation times, fluctuation amplitude and frequency do not produce significant differences in time-averaged quantities like velocity- or temperature-profiles. Both temperature- and velocity-profiles across the channel are shown in Fig.5, in the thermostatted steady state. For Nose-Hoover and velocity rescaling, the temperature profiles and velocity profiles are identical, showing a non-uniform profile, smallest in the middle and higher near to both walls. The velocity profile is almost (but not quite perfectly) a parabola, as expected from Poiseuille flow. For both thermostats, the dissipative force is proportional to the local particle velocity relative to the global center of mass (V-Vcm). The damping due to the relative velocity is strong in the middle, while heat is produced in the sheared regions with large velocity gradient close to the walls. This results in a temperature dip in the middle of the channel – and to small deviations from the parabolic flow profile expected for constant temperature.

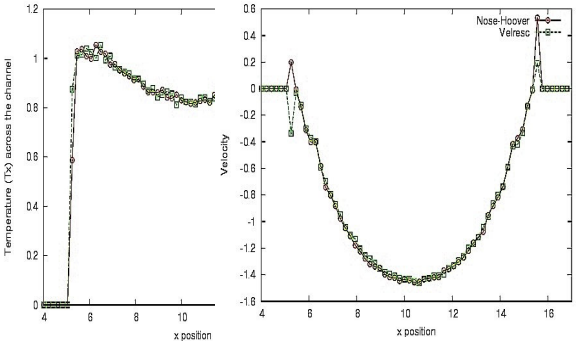

Fig.5: The left and right panels show the temperature- and velocity-profiles across the channel for body force bz=0.3. (The left panel shows only the left half of the system.) Circles and squares correspond to the Nose-Hoover and velocity rescaling methods, respectively.

Local (near-wall) thermostat

To obtain a more uniform temperature distribution across the channel, we use local thermostatting. The near wall region is divided into three bins, 1σ in width, along x-direction on both the sides, and the Nose-Hoover thermostat acts in each of them independently. Fig. 6 shows the temperature and velocity profiles in this case. We observe a nearly uniform temperature profile, slightly higher in the middle of the channel. The local thermostat leads to a different velocity profile from the 'global' one as shown in the right panel of figure 6. The velocity profile is sharper, more closely resembling a parabola.

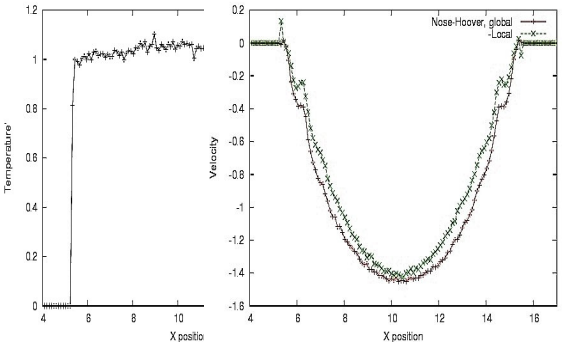

Fig.6: The left figure shows the temperature profile across the channel in case of local (near-wall) Nose-Hoover thermostat. The velocity profiles for local (x) and global (+) thermostats are shown on the right for body force bz=0.3.

Close to the wall, a discontinuous velocity gradient appears from the velocity profiles (Fig 6) - caused by

the near–wall layering, as also visible from the oscillatory density structures in Fig.1.

Local wall thermostat

Finally, one can implement a thermostat, which dissipates the heat through real wall-fluid interactions. In this model the wall atoms are mobile, they are allowed to move about their mean positions, and interact with the fluid atoms. For this, seven (fcc 001) wall layers have been used on each side – the two outermost layers are fixed particles, the five inner layers are mobile and thermostatted – whereas the fluid particles are not. A constant temperature T=1.0 is achieved at the wall with the Nose-Hoover thermostat.

In this case the fluid-fluid, fluid-wall and wall-wall interaction diameters and interaction strengths are taken as 1.0, 1.0, 0.8, and 1.0, 1.0, 10.0, respectively. The high wall-wall interaction strength is sufficient to prevent it from melting.

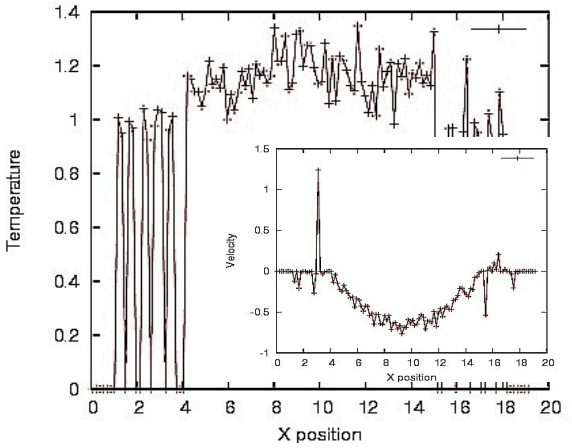

Fig.7: Temperature profile across the channel for wall-thermostatted Poiseuille flow with bz=0.1. Wall layers on both the side are maintained at a constant temperature 1.0. Fluid particles collide with the wall particles and dissipate their excess heat at the wall. *Inset*: Velocity profile across the channel. Averaging is over a few snapshots only, therefore the bad statistics.

The temperature- and velocity-profiles is shown in Fig. 7 for a body force with bz=0.1. There is an overall heating in the system due to insufficient dissipation at the wall, but it produces a more or less uniform distribution of temperature with slightly higher temperature in the fluid.

CONCLUSION

Poiseuille flow in a nano-slit of width ~11σ is simulated by molecular dynamics with a Lennard-Jones fluid. Different ways of thermostatting have been examined with the goal of a better understanding of the underlying dynamics.

The use of global thermostats leads to non-uniform temperature profiles, which can lead to “in-correct” (non-parabolic) velocity profiles and consequently to a inconsistent “measurement” of macroscopic hydro-dynamic quantities, like viscosity, when computed from the velocity profile [8]. Such artefacts (related to non-constant temperature) can be corrected by the use of local thermostatting or a wall thermostat, which both produce a much more uniform temperature distribution.

Thermostats affect the random thermal motion of the fluid particles. The global thermostats tested do not affect the velocity field in the channel. Local or wall thermostats do lead to different (more parabolic) velocity fields and to a much more homogeneous temperature across the slit.

The effect of the thermostats on single tracer particles is in progress. Fourier analysis did not show a strong difference for Nose Hoover and velocity rescaling when a single particle was examined (where the single particle was not affected by the thermostat). No peculiar frequencies are observed in the spectra.

ACKNOWLEDGEMENTS

We acknowledge MicroNed, the Dutch national programme for microtechnology research and innovation, for the financial support for our research. Also helpful discussions with J. Koplik, A. Markesteijn, and J. Westerweel are acknowledged.

REFERENCES

1. Allen M. P. & Tildesley D. J., 1987, Computer simulation of liquids, Oxford University Press Inc., New York.
2. Koplik J. & Banavar J. R., 1988, Molecular dynamics simulation of microscale Poiseuille flow and moving contact lines, *Phys. Rev. Lett.* ***60,*** 1282.
3. Thompson P. A. & Robbins M. O., 1990, Shear flow near a solid: Epitaxial order and flow boundary condition, *Phys. Rev. A* **41**, 6830.
4. Bitsanis, Ioannis, Somers, Susan A., H. Ted Davis, and MathewTirrel, 1990, Molecular Dynamics of flow in molecularly narrow pore, *J. Chem. Phys.,* **93**(5) 3427.
5. Fan X. J., Phan Thien N., Tong N. T. & Diao., X, Molecular dynamics simulation of a complex channel flow, *Physics of Fluids* **14**, 1146.
6. Eggers J., 2002, Dynamics of a nanojet. *Phys. Rev. Lett.* **89**, 084502.
7. Rudd Robert E. & Broughton Jeremy Q., 1998, Coarse-grained molecular dynamics and the atomic limits of finite elements, *Phys. Rev. B* **58** (10) R5893.
8. Ghosh, A., Luding, S., 2007, in preparation.